Pd Nanoparticles supported on Silver, Zinc, and Reduced Graphene Oxide as a Highly Active Electrocatalyst for Ethanol Oxidation

Nagesh D. Pawar[a], *Christopher J Barile*[b], *Jagdish C. Bhangoji*[a], *Ashok G. Awale*[a], *and Suresh S. Shendage**[a]

[a]Department of Chemistry, KET'S V. G. Vaze Kelkar College, Mithagar Road, Mulund (E), Mumbai-400081, Maharashtra (India).

[b]Department of Chemistry University of Nevada, Reno, Reno, NV, USA.

*Corresponding author:sureshsshendage@gmail.com

Abstract

In this manuscript, we present a facile approach to synthesize a highly active catalyst for the electro-oxidation of ethanol using Pd nanoparticles supported on a Ag-Zn alloy on reduced graphene oxide. This nanocomposite material was fabricated via a two-step process of incineration followed by sol-gel synthesis. The physical properties of the catalyst were evaluated using X-ray diffraction, X-ray photoelectron spectroscopy, and scanning and transmission electron microscopies. To understand the catalyst's activity for ethanol oxidation, we performed a series of cyclic voltammetry and electrochemical impedance spectroscopy experiments in alkaline medium. The catalyst exhibited excellent catalytic activity with a current density of 13.01 mA cm^{-2}, a value seven times higher than the commercial standard Pd/C catalyst and higher than any other previously reported Pd-based catalyst. The results were attributed synergistic effects between the Pd and alloy support along with the large electrochemically active surface area of the material. Taken together, these results suggest that ethanol electrocatalysts based on nanocomposites of Pd, Ag, and Zn are promising candidates for future ethanol fuel cells.

Keywords: Pd nanoparticles, ethanol, electrocatalyst, cyclic voltammetry, fuel cells.

1. Introduction

Our reliance on fossil fuels for the global energy economy is unsustainable and is the major contributor to global climate change. The pursuit of efficient, renewable, and environmentally-friendly alternative energy sources and conversion processes is therefore of paramount interest.[1] Fuel cells offer a highly effective pathway for transforming chemical potential energy into electrical energy.[2-3] Fuel cells can employ a wide range of fuels. Among the various fuel cells investigated, direct alcohol fuel cells (DAFC) have attracted significant research attention due to their high efficiency, minimal environmental impact, low noise, high reliability, and ease of maintenance. Additionally, like their more prevalent H_2 fuel cell counterparts, DAFCs can be used as power sources in electric vehicles due to their high energy densities [4-8]. Consequently, these attributes have brought significant interest among the scientific community and scholars.

Both methanol and ethanol can be considered for use in DAFCs. Methanol is generally considered more promising than ethanol due to its lower working temperature and higher overall module efficiency. The higher fuel cell efficiency results from the fact that the electrochemical oxidation of methanol is generally faster than that of larger alcohols.[9] However, the lower energy density of methanol along with its poisonous nature present two substantial challenges.[10] On the other hand, the use of ethanol in fuel cells offers several benefits because it is nontoxic, possesses a high fuel density (8 kWh kg^{-1}), produces less harmful by-products upon oxidation, and can be straightforwardly produced from biomass. When ethanol is fully oxidized to CO_2, it yields a relatively high output of twelve electrons per molecule.[11] These characteristics make ethanol a compelling choice for fuel cells [12-14].

Challenges associated with direct ethanol fuel cells (DEFCs) include the need for suitable cell membranes and sluggish anode reaction kinetic. To address the latter challenge, it is imperative to create an electrocatalyst that exhibits high catalytic activity and long-term stability for ethanol oxidation.[13,14] Noble metal nanoparticles have been employed extensively for DAFC catalysts due to several useful and tuneable properties. Pt-based catalysts have been thoroughly studied for use in methanol and ethanol electro-oxidation. However, Pt-based catalysts suffer from various drawbacks including high cost and reduced stability due to susceptibility to poisoning by intermediates like CO and Cl^-. These limitations have restricted the scope of catalytic applications for alcohol oxidation.[15]

To resolve these issues, Pd-based catalysts have been widely employed as substitutes for Pt-based anode catalysts owing to advantages such as lower cost, lower sucestibility, and significant electro-catalytic activity towards alcohol oxidation in alkaline medium.[16] Nonetheless, particle aggregation due to Ostwald ripening decreases long-term stability and lowers catalytic activity in these systems.[17] Hence, various support materials have been tested in attempts to maintain a uniform dispersion of nanoparticles. An assortment of carbon-containing support materials such as carbon nanofibers,[18] carbon nanotubes,[19-20] Vulcan XC-72 carbon black,[21-22], and condensed graphene oxide[23-24] have been used to support Pd nanoparticles. Carbon supports frequently offer a large surface area, result in relatively small nanoparticles, and enable highly conductive materials. In addition to carbons, metal oxides including TiO_2,[25] NiO, [26], CeO_2, Co_3O_4,[27] and SnO_2,[28] a carbon nanotube-encapsulated NiO/MgO,[29] a Mg-Al-CO_3 incrusted dual hydroxide,[30], a ternary Al-Mg-Ag alloy[31] have also been investigated as support materials, which can significantly improve the activity of Pd nanocatalysts for ethanol oxidation. Alloys not only decrease the noble metal loading, but they noticeably modify the electronic properties of catalytic materials.[32] This change in electronic properties due to the multiple components in alloys alters the % d band character of elements, which can accelerate the rate of adsorption, bond breaking and bond making events during catalysis.[33-34]

In previous reports, various bimetallic and multimetallic catalysts including PdNi,[35] PdFe,[36] PdCu,[37] PtPdAg/C,[38] CoAuPdPt,[39] Au@PdAg,[40] and AlMgAg[41] have been studied due to various synergistic effects, which enhance the rate of ethanol oxidation in basic medium. Additionally, owing to its good electrical, optical, and mechanical properties, graphene has been investigated for a host of different applications.[42-43] In 1958, Hummer and Offeman established a biochemical technique to manufacture graphene oxide by acidic processing of graphite.[44] Pallellappa et al. subsequently developed a convenient and fast method for synthesizing reduced graphene oxide (rGO) nanosheets by the direct decomposition of sugar, without the use of any toxic solvents, metal catalyst, or hazardous reagents.[45] In this work, we study the use of a ternary nanocomposite (Ag-Zn-rGO) as a support for the growth of Pd nanoparticles to create a highly active electrocatalyst for ethanol oxidation alkaline medium. The synthesis of this catalyst and its electrochemical application towards ethanol oxidation is illustrated in **Scheme 1**.

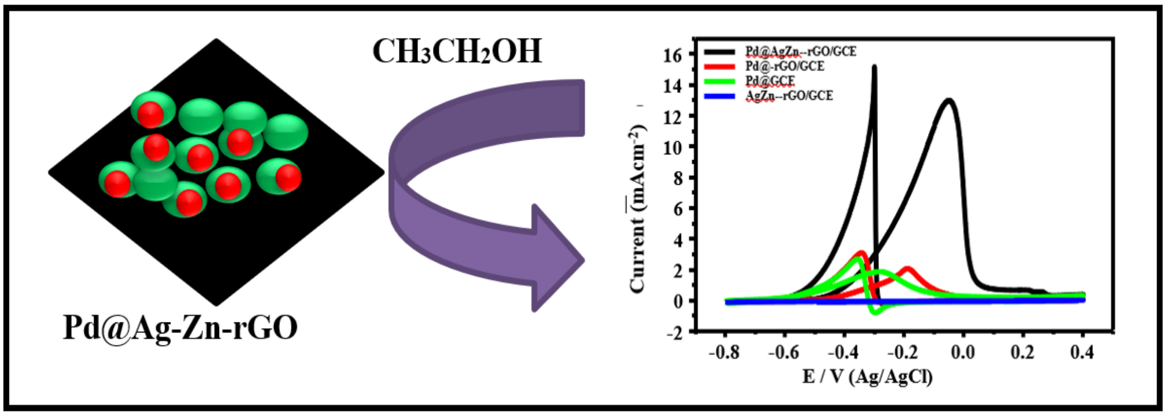

Scheme 1. Pd@Ag-Zn-rGO synthesis and its application for ethanol electro-oxidation.

2. Experimental

2.1. Materials

All chemicals including sucrose, commercial Pd/C powder, ethanol, HCl, H_2SO_4, $PdCl_2$, Whatman paper-41, Ag, Zn metal powder, NaCl salt, 5 wt. % Nafion solution, 0.05 and 0.3 µm alumina powder, glassy carbon electrode (3 mm) were A.R. grade and used without any further purification.

2.2. Instrumentation

Morphological and structural information was investigated using scanning electron microscopy (SEM, JSM-6360LA), transmission electron microscopy (TEM, JSM-6360LA), and X-ray diffraction (XRD, JSM-6360LA) techniques. Electrochemical properties were examined using EIS, cyclic voltammetry (CV), chronoamperometry using a PGSTAT 302N potentiostat from Auto Lab.

2.3. Preparation of Ag-Zn-rGO Support

A rapid solidification method was used to prepare the Ag-Zn-rGO alloy. In a typical procedure, 1 g of Ag metal powder, 1 g of Zn metal powder, and 4 g of sucrose was placed in a silica crucible and mixed thoroughly. The mixture was then gently heated in a muffle furnace at 700 ^{0}C for 5 hrs and immediately quenched in 30 wt. % brine solution. Subsequently, the product was dried in an oven and grounded to a fine powder using a mortar and pestle.

2.4. Preparation of Pd@Ag-Zn-rGO Catalyst

0.4 g of the previously synthesized Ag-Zn-rGO alloy was placed in a 100 mL beaker containing 10 mL of distilled water and sonicated for 10 min. Next, 0.2 g of $PdCl_2$ was placed in another beaker containing 10 mL of distilled water and 3 mL of conc. HCl, and the resulting mixture was sonicated for 10 min. Consequently, the solution from the second beaker was carefully transferred into the first beaker. Then, 3 mL of hydrazine hydrate was added slowly to this reaction precursor, and the mixture was vigorously stirred for 2 hrs at 90 ^{0}C. Afterwards, the precipitate was collected via filtration and carefully washed with distilled water followed by ethanol. Finally, the material was dried in an oven at 110 ^{0}C for 2 hrs.

2.5. Preparation of Pd@Ag-Zn-rGO/GCE Modified Electrode

To prepare a catalyst ink, 5 mg of the synthesized catalyst was dispersed in 1 mL of a mixture containing distilled water, ethanol, and Nafion solution using an ultrasonic bath for

30 min. Before modification of the glassy carbon electrode (GCE), the electrode was thoroughly polished using 0.5 and 0.03 µm alumina slurries to achieve a mirror-like finish. Subsequently, the electrode was rinsed with distilled water and subjected to ultrasonic cleaning in ethanol for 5 min. Next, a 10 µL drop of the prepared ink was cast on the surface of previously cleaned GCE electrode followed by drying at room temperature. This modified GCE electrode was then used for further studies involving ethanol electro-oxidation.

2.6. Electrochemical Characterization

The electrochemical performance of the newly synthesized catalyst was thoroughly assessed using a three-electrode system at an electrochemical workstation operated via NOVA 2.1 software and a standard cell setup consisting of a Ag/AgCl reference electrode, a Pt wire counter electrode, and a modified GCE working electrode. The experimental measurements were carried out in 1 M NaOH and 1 M ethanol solution over a potential range between 0.4 to 0.8 V vs. Ag/AgCl at a scan rate of 50 mV/s. Moreover, chronoamperometric measurements were recorded at a constant applied potential of 0.2 V for a duration of 1,000 s. For electrochemical impedance spectroscopy (EIS) analysis, experiments were performed at a potential of 0.3 V with an amplitude of 10 mV and a frequency range of 10^{-2} to 10^{6} Hz.

3. Results and Discussion

3.1. Structural and Morphological Characterization

Before evaluating the Pd@Ag-Zn-rGO/GCE electrocatalyst for its ability to oxidize ethanol, we first characterized the synthesized catalyst using a suite of techniques. The XRD spectrum indicates the presence of a diffraction peak at $2\theta^{o} = 27.0$, which is assigned to rGO. The diffraction peaks around $2\theta^{o} \approx 40.1, 46.5, 68.2$ correspond to the Pd (111), (200), and (220) crystal planes, respectively, which match what is expected for the face centred cubic (FCC) crystalline planes of Pd (**Fig. 1**).[46] Diffraction peaks at 38.1^{o}, 44.4^{o}, 64.8^{o}, 77.7^{o}, and 80.1^{o} correspond to the (111), (200), (220), (311), and (222) lattice planes of the Ag nanoparticles, respectively.[47] Additionally, the diffraction peaks observed at 33.9° and 54.9° are due to a tetragonal PdO phase and are indexed to the (100) and (110) crystal planes, respectively (JCPDS#85-0713).[48] The XRD peaks at 36.3°, 39.1°, 43.3°, 54.4°, 70.1°, 70.7° and 77.0° are assigned to the (002), (100), (101), (102), (103), (110), and (004) HCP planes of Zn nanoparticles, respectively, and match those found in JCPDS file 00-004-0784.[49] Similarly, the (002) diffraction peak at 34.2° reveals that relatively little amount of Zn metal was converted to hexagonal wurtzite ZnO nanocrystals during the heating step during the synthetic scheme.[50]

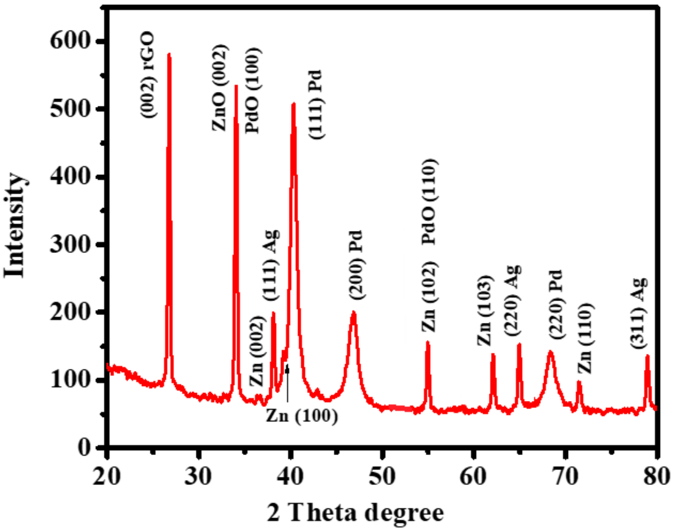

Figure 1: X-ray diffraction (XRD) pattern of as-synthesized Pd@Ag-Zn-rGO.

Next, we performed XPS to characterize the elemental composition and local bonding environment of the as-prepared catalyst. A survey scan across a wide range of binding energies reveals the presence of C, O, Zn, Pd, and Ag in the catalyst (**Fig. 2A**). While most of the peaks are well resolved, the Pd $3p_{3/2}$ peak directly overlaps with the O 1s peak, which hinders a high-resolution analysis of the O 1s region.[51] Among C, Zn, Pd, and Ag, the relative atomic percentages from XPS analysis are calculated to be 78.2%, 10.8%, 10.1%, and 0.8%, respectively. **Fig. 2B** displays the high-resolution XPS scan of the C 1S region. The spectrum possesses a prominent peak at 284.7 eV, which is ascribed to C-C bonding. The tail of the peak at binding energies greater than 285 eV can be fit to three peaks with binding energies of 287.1 eV, 288.4 eV, and 289.5 eV, which are due to C-O, C=O, and O-C=O bonding environments, respectively. All of these bonding environments are typical for rGO, and the peak positions match those reported previously.[52] Furthermore, the Zn XPS spectrum possesses two peaks at 1022.9 eV and 1046.1 eV, which correspond to the Zn $2p_{3/2}$ and Zn $2p_{1/2}$ transitions, respectively (**Fig. 2C**). The high-resolution Pd XPS spectrum can be fit to four peaks (**Fig. 2D**). The two most intense peaks at 335.2 eV and 340.4 eV are Pd metal peaks due to the Pd $3d_{5/2}$ and Pd $3d_{3/2}$ transitions, respectively. A set of less intense peaks at 337.0 eV and 342.3 eV are due to PdO that correspond to analogous transitions. These results indicate that some of the Pd in the catalyst was converted to PdO during synthesis. Lastly, the Ag XPS spectrum contains two peaks at 367.4 eV and 373.3 eV, which are assigned to the Ag $3d_{5/2}$ and Ag $3d_{3/2}$ transitions, respectively (**Fig. 2E**). The signal-to-noise of the high-resolution Ag spectrum is relatively poor due to the low quantity of Ag used to prepare the catalyst.

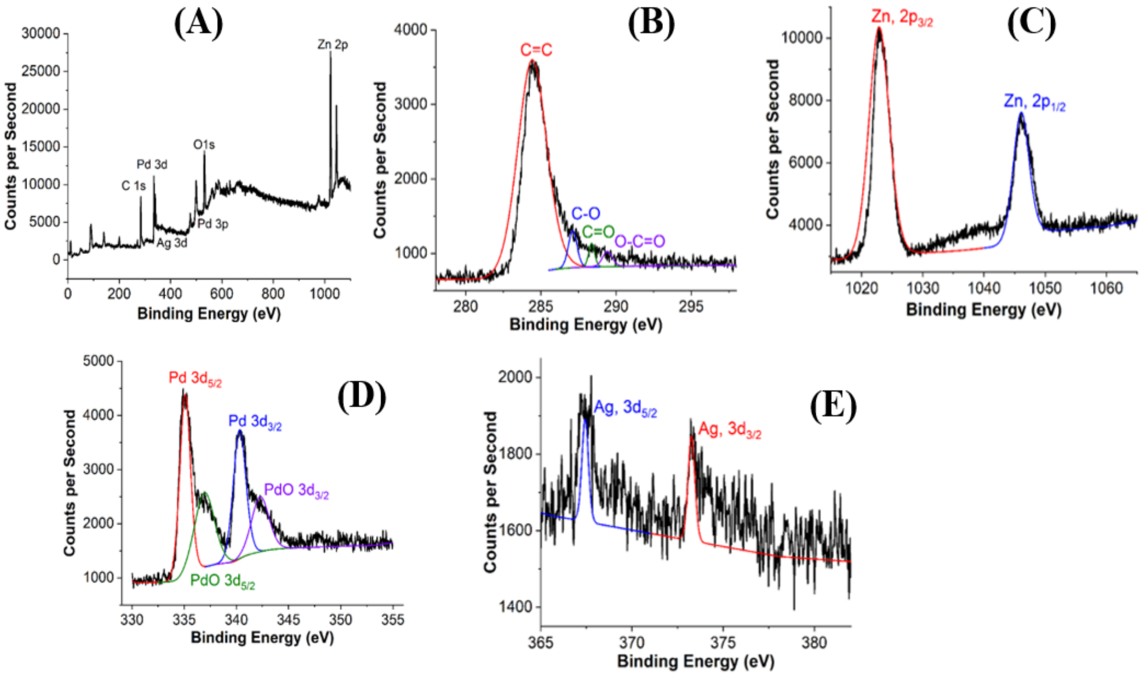

Figure 2: XPS spectra of the as-prepared catalyst: survey scan **(A)** and high-resolution scans of C **(B)**, Zn **(C)**, Pd **(D)**, and Ag **(E)**.

Morphological information of Pd@Ag-Zn-rGO catalyst was investigated by scanning electron microscopy (SEM) and transmission electron microscopy (TEM). The catalyst consists of Pd nanoparticles uniformly dispersed over the surfaces of the Ag-Zn-rGO support (**Fig. 3A**).The smooth and uniform texture along with the large surface area of the Ag-Zn-rGO support enables the uniform dispersion and high loading of Pd nanoparticles. **Fig. 3B** displays the TEM image of the catalyst and shows the distribution of the Pd NPs across the support. The relatively small Pd NPs are highly loaded and dispersed on the surface of the Ag-Zn-rGO support, which is consistent with the information gleaned from SEM analysis. The particle size and average diameter of Pd NPs were found to be in the range of 11 to 38 nm and 15 nm, respectively. The highly crystalline nature and FCC structure of the Pd NPs were further confirmed by the appearance of bright ring patterns in selected area electron diffraction (SAED) analysis (**Fig. 3C**). The EDS spectrum (**Fig. 3D)** of the Pd/Ag-Zn-rGO electrocatalyst confirms the presence of Pd along with Ag, Zn metal, and C from the rGO. Taken together, these characterization techniques indicate that the targeted nanocomposite catalyst was successfully synthesized.

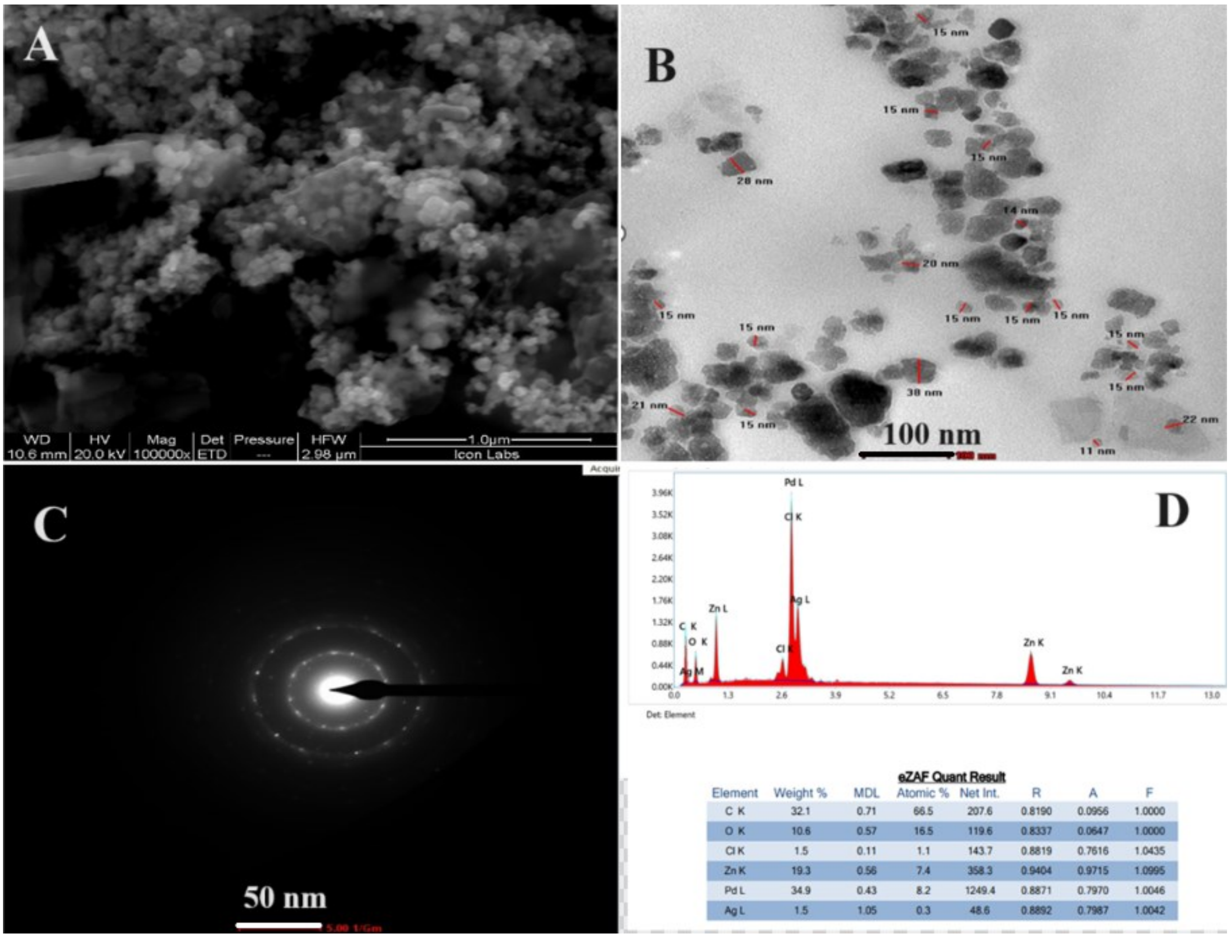

eZAF Quant Result

Element	Weight %	MDL	Atomic %	Net Int.	R	A	F
C K	32.1	0.71	66.5	207.6	0.8190	0.0956	1.0000
O K	10.6	0.57	16.5	119.6	0.8337	0.0647	1.0000
Cl K	1.5	0.11	1.1	143.7	0.8819	0.7616	1.0435
Zn K	19.3	0.56	7.4	358.3	0.9404	0.9715	1.0995
Pd L	34.9	0.43	8.2	1249.4	0.8871	0.7970	1.0046
Ag L	1.5	1.05	0.3	48.6	0.8892	0.7987	1.0042

Figure 3: **(A)** SEM, **(B)** HR-TEM, **(C)** SEAD pattern, and **(D)** EDX analysis of the Pd@Ag-Zn-rGO catalyst.

3.2. Electrochemical Performance

To evaluate the electrocatalytic performance of the synthesized Pd@Ag-Zn-rGO material, electrochemical experiments were conducted in 1 M NaOH and ethanol solution in the potential window of -0.8 V to +0.4 V vs. Ag/AgCl at a scan rate of 50 mV/s (**Fig. 4A** and **4B**). As can be seen from **Fig. 4A**, the Pd@Ag-Zn-rGO catalyst-modified electrode exhibited a shoulder at E_p = 0.25 V due to the generation of both PdO and Ag_2O during the anodic scan. In the cathodic scan, two peaks are observed at E_p = -0.025 V and E_p = -0.47 V (black line), which confirms the reformation of Pd and Ag NPs from these oxidized species.[53-55]

The peak associated with the transformation of PdO into Pd was employed to calculate the electrochemically active surface area (EASA), which was determined using the following equation:

EASA = Q/SI

In this equation, *Q* represents the Coulombic charge associated with the reduction of PdO, *S* stands for the proportionality constant, and *I* denotes the Pd loading in grams. For the reduction of the PdO monolayer, a charge value of 0.405 mC cm^{-2} was assigned as has been used previously in EASA calculations.[56] The calculated EASA value for the Pd@Ag-Zn-rGO modified electrode was found to be 1.29 cm^2 mg^{-1} of Pd which is 2.1 times higher than that of the standard commercial Pd/C catalyst, which has an EASA of 0.62 cm^2 mg^{-1}.

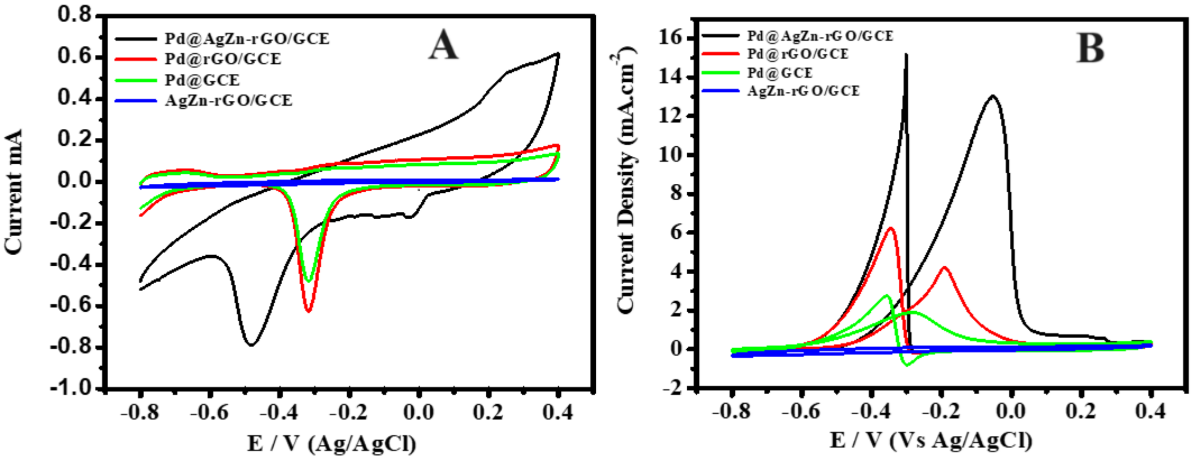

Figure 4: The CVs of various modified electrodes in 1 M NaOH solution **(A)** and 1 M ethanol +1 M NaOH **(B)** at an applied potential of -0.8 to 0.4 V and a scan rate of 50 mV s^{-1}.

In the presence of ethanol, the forward and backward scans of the Pd@Ag-Zn-rGO catalyst correspond to the oxidation of ethanol and adsorbed carbonaceous species like CO, respectively.[56] The onset and peak potential values of the catalyst are E_{onset} = -0.632 V and E_p = -0.012 V for ethanol oxidation (**Fig. 4B**), which are indicative of good catalytic behavior of the synthesized material and better than that of the standard commercial Pd/C (20%) catalyst (E_{onset} = -0.547 V and E_p = -0.187 V).

The Pd@Ag-Zn-rGO composite modified electrode exhibited a significantly higher peak current density of 13.01 mA cm^{-2}, which is seven times greater than Pd/C (1.84 mA cm^{-2}). The ratio of the forward to backward peak current density (i_f/i_b) is a useful indicator of the catalyst's resistance to poisoning. For the Pd/Ag-Zn-rGO catalyst, the ratio was found to be 0.925, which is higher than that of Pd/C (0.676) under similar reaction conditions.

Together, these results demonstrate that several attributes of the Pd/Ag-Zn-rGO catalyst render it superior to the commercial Pd/C (20%) catalyst for ethanol electro-oxidation. This superior performance is attributed to the enhanced active surface area and synergistic effect of the alloy material, which improves the ability of the catalyst to oxidize ethanol and carbonaceous intermediates.

The catalytic performance of the synthesized composite material for ethanol oxidation was compared with previously reported Pd-based catalysts (**Table 1**). These results reveal that the synthesized catalyst exhibits one of the most negative onset potentials for ethanol electro-oxidation as well as the highest current density reported, indicating that the Pd/Ag-Zn-rGO catalyst represents a significant step forward in the state of the art and is a promising candidate for practical ethanol electro-oxidation.

Table. 1. Comparison of different catalysts used in electro-oxidation of ethanol.

Electrode	Electrolyte Solution	Onset Potential (V)	Peak potential (V)	Current Density (mA.cm^{-2})	Ref.
FeCo@Fe@Pd	0.5M KOH +0.5 M Ethanol	-0.71	-0.28	3.93	[57]
Pd/Ni@N-rGO	1M KOH +1 M Ethanol	-0.48	-0.143	0.69	[58]
NiNW/PdNFs	0.5M KOH + 1M Ethanol	-0.5	-0.09	0.15	[59]
PdSnAg/C	1M KOH + 1M Ethanol	-0.52	-0.17	3.37	[60]
AuPd NWs/LDH-CB	1.0 M KOH + 1.0 M ethanol	-0.50	-0.15	12.44	[61]
Cu@Pd core shell	2.0 M KOH + 3.0 M ethanol	-0.60	0.11	6.78	[62]
Pd@Ag-Zn-rGO	1M NaOH+1 M Ethanol	-0.632	-0.012	13.01	Present Work

3.3. Catalyst Stability

The study of long-term durability of the modified electrode is an important property to validate electrocatalytic performance of the synthesized catalyst for the electrooxidation of ethanol. **Fig. 5** demonstrate chronoamperometric (*i-t*) curves for Pd@AgZn-rGO/GCE, Pd@rGO/GCE, and Pd@GCE in a solution containing 1 M NaOH and 1 M ethanol at an applied constant potential of 0.2 V for 1,000 s. As shown in **Fig. 5**, the Pd@AgZn-rGO composite electrode possesses greater retention of current density throughout the entire duration of the experiment as compared to the other fabricated electrodes. These experiments revealed that the synthesized material has excellent stability over 1,000 s, at least compared to the standard Pd catalysts.

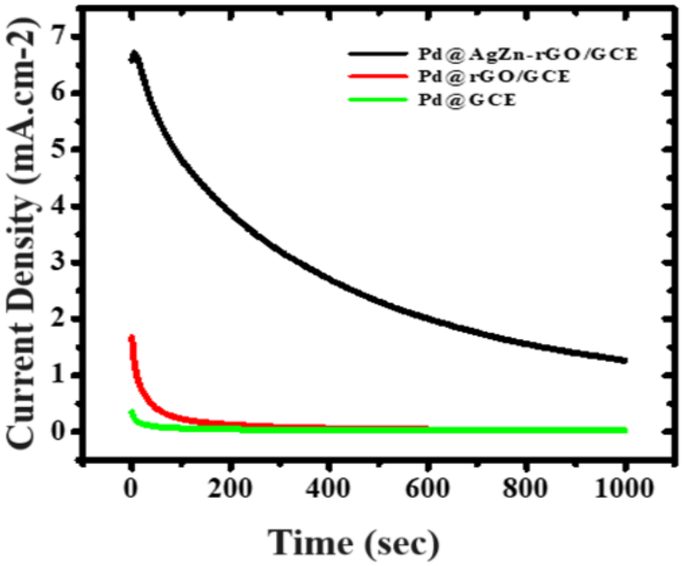

Figure 5: Chronoamperometry (*i-t*) curves of Pd@Ag-Zn-rGO, Pd@rGO and Pd@GCE modified electrodes in a solution containing 1 M NaOH and 1 M ethanol at -0.2 V for 1,000 s.

3.4. EIS Measurements

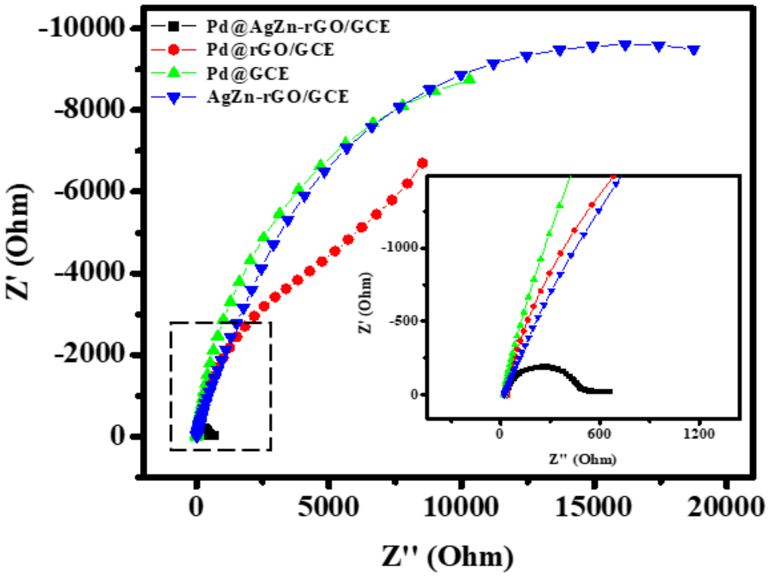

Figure 6: Nyquist Plot of Pd@Ag-Zn-rGO,Pd@rGO, Pd@Cand Ag-Zn-rGO in a solution containing 1 M NaOH and 1 M ethanol at 0.3 V and 10 mV amplitude with a frequency range from 10^{-2} to 10^{6} Hz.

We used electrochemical impedance to investigate the charge transfer resistance of the catalytic material ethanol electro-oxidation. The diameter of the semicircle is an essential property used to determine the chargetransfer resistance (R_{ct}) of a catalyst.[63] Nyquist plots of various modified electrodes were examined in a solution containing 1 M NaOH and 1 M ethanol solution at a potential of 0.3 V with a frequency range from 10^{-2} to 10^{6} Hz. As shown in **Fig. 6**, the Pd@Ag-Zn-rGO modified electrode displayed a smaller arc diameter which indicates that Pd@Ag-Zn-rGO catalyst exhibits lower charge transfer resistance (R_{ct}) and rapid electron transfer at the catalyst surface. These properties enhance the electro-catalytic performance towards oxidation of ethanol, which is consistent with above results.

4. Conclusions

In summary, we successfully synthesized a Pd@Ag-Zn-rGO catalyst using a facile incineration and sol-gel approach using hydrazine as a reducing agent. The obtained Pd NPs were uniformly deposited and dispersed over the surface of the Ag-Zn-rGO support. The fabricated composite was characterized by various techniques including XRD, XPS, SEM, TEM, and EDX. The electrical conductivity was modified by alloying and the interface with reduced graphene oxide. The alloyed material played an important role in improving electron transfer rate and poisoning resistance. Consequently, the synthesized Pd@Ag-Zn-rGO composite exhibited excellent catalytic activity with significantly higher current density towards ethanol electro-oxidation than previously reported Pd-based materials. Furthermore, the resultant current density of the catalyst was found to be seven times greater compared to the commercial Pd/C catalyst. The prepared Pd@Ag-Zn-rGO nanocomposite showed excellent electrocatalytic activity and stability towards ethanol oxidation in alkaline medium. Thus, this work provides a new facile strategy to prepare a supported material with higher catalytic performance towards ethanol oxidation by anchoring Pd NPs on a hybrid support material.

Declaration of Competing Interest

The authors declared that they have no any competing interests or personal relationships that could influence the work reported in this paper.

Author contributions

Nagesh D. Pawar: carried out the experimental work and writing the manuscript, **Dr. Christoper Barile:** data analysis, interpretation of results, and editing the manuscript. **Dr. Jagdish C. Bhangoji:** data analysis, interpretation of results, and editing the manuscript, **Ashok G. Awalae:** review and editing of the manuscript **Dr. Suresh S. Shendage:** conceptualization and correction of the manuscript, All authors gave final approval for publication.

Acknowledgements

The authors are thankful laboratory staff for providing facilities to complete this work. C.J.B. acknowledges support from the National Science Foundation CAREER Award under Grant No. CHE-2046105